CO_2-Facilitated Transport Through Poly(*N*-vinyl-γ-sodium aminobutyrate-*co*-sodium acrylate)/Polysulfone Composite Membranes

Zhi Wang, Chunhai Yi, Ying Zhang, Jixiao Wang, Shichang Wang

Chemical Engineering Research Center, School of Chemical Engineering and Technology, Tianjin University, Tianjin, 300072, China

Received 23 November 2004; accepted 20 June 2005
DOI 10.1002/app.23100
Published online in Wiley InterScience (www.interscience.wiley.com).

ABSTRACT: Poly(*N*-vinyl-γ-sodium aminobutyrate-*co*-sodium acrylate) (VSA–SA)/polysulfone (PS) composite membranes were prepared for the separation of CO_2. VSA–SA contained secondary amines and carboxylate ions that could act as carriers for CO_2. At 20°C and 1.06 atm of feed pressure, a VSA–SA/PS composite membrane displayed a pure CO_2 permeation rate of 6.12×10^{-6} $cm^3(STP)/cm^2$ s cmHg and a CO_2/CH_4 ideal selectivity of 524.5. In experiments with a mixed gas of 50 vol % CO_2 and 50 vol % CH_4, at 20°C and 1.04 atm of feed pressure, the CO_2 permeation rate was 9.2×10^{-6} cm^3 (STP)/cm^2 s cmHg, and the selectivity of CO_2/CH_4 was 46.8. Crosslinkages with metal ions were effective for increasing the selectivity. Both the selectivity of CO_2 over CH_4 and the CO_2 permeation rate had a maximum against the carrier concentration. The high CO_2 permeation rate originated from the facilitated transport mechanism, which was confirmed by Fourier transform infrared with attenuated total reflectance techniques. The performance of the membranes prepared in this work had good stability. J Appl Polym Sci 100: 275–282, 2006

Key words: gas permeation; membranes

INTRODUCTION

The separation and removal of CO_2 are required in many areas, such as the upgrading of natural gas, landfill gas recovery, and enhanced oil recovery. The membrane separation method is particularly attractive in comparison with conventional separation methods such as absorption, adsorption, and cryogenic distillation because of the low capital required, high-energy efficiency, and environmental friendliness.[1,2] Usually, commercially available polymeric membranes have either high permeability or high selectivity, but not both.[3] However, facilitated transport membranes (including supported liquid membranes, ion-exchange membranes, and fixed carrier membranes) selectively permeate CO_2 by means of the reversible reaction between CO_2 and the carriers in the membranes, so they possess high permeability as well as high selectivity.[4] Although supported liquid membranes and ion-exchange membranes show remarkably high performance, they are unstable.[5–8] A fixed carrier membrane, in which the carrier is chemically bound, may be unique in providing stability as well as both high permeability and selectivity.

In recent years, fixed carrier membranes for CO_2 separation with facilitated transport groups (amine moieties) have been investigated extensively.[6–9]

In this work, poly(*N*-vinyl-γ-sodium aminobutyrate-*co*-sodium acrylate) (VSA–SA) was prepared by the hydrolysis of the copolymer of *N*-vinylpyrrolidone (NVP) and acrylamide (AAm). The composite membranes were developed with VSA–SA as the active layer and a polysulfone (PS) ultrafiltration membrane as the support. VSA–SA has a secondary amine and a carboxylate ion, which can reversibly react with CO_2[10,11] and thus can be expected to act as carriers for CO_2. Furthermore, because VSA–SA is highly hygroscopic, the humidified membranes can form a jell, which is beneficial to gas diffusion. Thus, such membranes have the potential for a high CO_2 permeation rate (R_{CO2}) and high selectivity.

EXPERIMENTAL

Materials

The copolymer of NVP and AAm was synthesized through radical polymerization in a 5 wt % monomer aqueous solution, which consisted of NVP (purified by fractional distillation under reduced pressure) and

Correspondence to: Z. Wang (wangzhi@tju.edu.cn).
Contract grant sponsor: National Basic Research Program; contract grant number: 2003CB615703.
Contract grant sponsor: Sinopec Corp.; contract grant number: X502010.

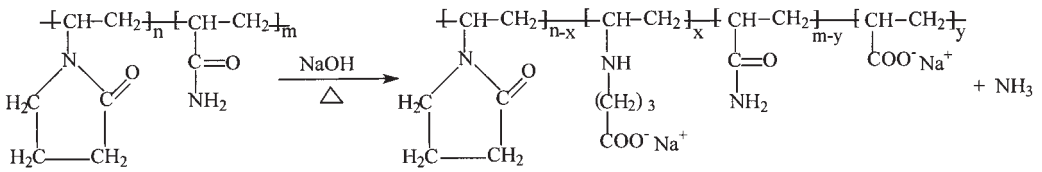

Figure 1 Equation of the hydrolysis reaction.

AAm, with azobisisobutyronitrile (twice recrystallized from ethanol) as the initiator at 49°C in an inert atmosphere of nitrogen gas.[12] The NVP–AAm copolymer was hydrolyzed in a sodium hydroxide solution. The hydrolysis reaction is shown in Figure 1. The liberated ammonia was carried away by a constant stream of nitrogen and absorbed in 100 mL of 0.1 mol/L HCl. The resulting polymer, VSA–SA, was precipitated with acetone, and then the VSA–SA aqueous solution was purified with an ion-exchange resin to remove low-molecular-weight impurities. PS support membranes (average molecular weight cutoff = 50,000) were purchased from the Research Center for Eco-Environmental Sciences of the Chinese Academy (Beijing, China).

Analytical experimentation

The composition of the NVP–AAm copolymer was determined by elemental analysis. An Elementar Vario EL (Germany) was used to determine the carbon, hydrogen, and nitrogen concentrations of the copolymer. The concentration of polyacrylate sodium in VSA–SA was calculated according to the amount of liberated ammonia obtained by the titration of redundant HCl. The total concentration of carboxylate ions was obtained through the titration of VSA–SA, as shown in Figure 2; the total concentration of carboxylate ions equaled that of consumed hydrochloric acid between two abrupt points. The concentration of poly(*N*-vinyl-γ-sodium aminobutyrate) in VSA–SA was calculated from the concentration of total carboxylate ions and polyacrylate sodium, and then the total carrier concentration was obtained. The crystallinity and interchain displacement (*d*-spacing) were determined with a wide-angle X-ray diffractometer (D/max-2500, Rigaku, Tokyo, Japan).

Membrane preparation and testing

An aqueous solution of VSA–SA was cast onto support membranes with an applicator and was dried at room temperature. The composite membranes were crosslinked in an aqueous solution of a metal salt (0.1 mol/L) for 1 min. The gas permeation of the membranes was measured with a set of test apparatus. The effective area of the composite membranes used in the test cell was 19.26 cm^2. Before coming into contact with the membrane, both the feed gas and the sweep gas (H_2) were passed through gas bubblers containing water. The outlet sweep gas composition was analyzed by a gas chromatograph equipped with a thermal conductivity detector (HP4890, Porapak N, Agilent, Wilmington, DE). The fluxes of CO_2 and CH_4 [cm^3(STP)/cm^2 s] were calculated from the sweep gas flow rate and its composition. The downstream pressure in the apparatus was 1 atm. The permeation rate and selectivity of CO_2 over CH_4 were given by $R_i = N_i/\Delta P_i$ and $\alpha = R_{CO2}/R_{CH4}$, respectively, where N_i is the flux, ΔP_i is the pressure difference between the upstream and downstream sides of the membrane (cmHg), and R_{CH4} is the permeation rate of CH_4.

RESULTS AND DISCUSSION

Permselectivity of the composite membrane

Figures 3 and 4 show the effects of the feed gas pressure on the performance of a VSA–SA/PS composite membrane with pure CO_2 or CH_4 and a mixture of 50 vol % CO_2 and 50 vol % CH_4 as the feed. The membrane possessed high R_{CO2} and α values. A comparison of these values with those of other fixed carrier membranes reported in the literature is shown in Table I. Although the membrane in ref. 6 showed a high permeation rate, which is an advantage of a plasma-

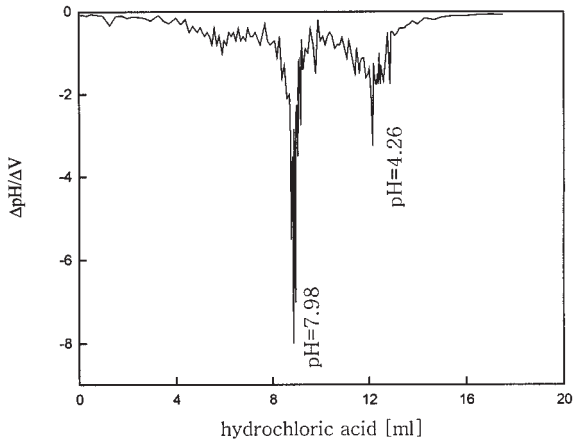

Figure 2 Titration curve of the hydrolysate of the copolymer. ΔpH/ΔV is the slope of titration curve, and can be defined as $\Delta pH/\Delta V = \partial(pH)/\partial(V)$, where V is the volume of hydrochloric acid.

polymerized membrane, its selectivity was only 11.5. The other membranes showed higher selectivity, but R_{CO2} could reach only 10^{-6} to 10^{-5} $cm^3(STP)/cm^2$ s cmHg; sometimes it was even 10^{-9} to 10^{-8} $cm^3(STP)/cm^2$ s cmHg. Therefore, from a comprehensive view, the performance of the composite membrane prepared in this work was better.

Figures 3 and 4 show that α with the mixed feed gas was much less than that with the pure feed gas. This was due to coupling effects between CO_2 and CH_4.[13]

Analysis of CO_2 transport in the membrane

The high R_{CO2} value of the composite membrane in this work was caused by the two kinds of carriers, the secondary amine and carboxylate ions, which facilitated the transport of CO_2. The transport mechanism of CO_2 was characterized by Fourier transform infrared (FTIR; Nicolet Magna-IR, Madison, WI) with attenuated total reflectance techniques. Membranes in different states were investigated, as shown in Figure 5. In comparison with the blank membrane, the humidified membrane absorbing CO_2 resulted in the appearance of several new bands: 2543, 1922, 1400, and 997 cm^{-1}. The bands at 2543 and 1922 cm^{-1} could be attributed to the complex of CO_2 and active groups. The bands at 1400 and 997 cm^{-1} could be attributed to HCO_3^-. These bands disappeared in the spectrum of the aforementioned membrane after desorption. Therefore, CO_2 could react reversibly with the membrane. Although the spectrum of the humidified mem-

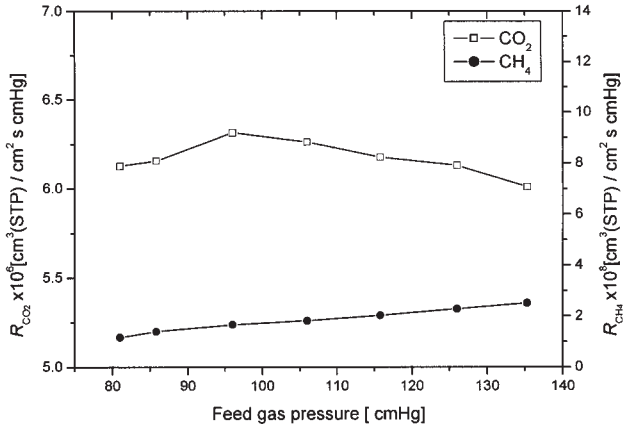

(a)

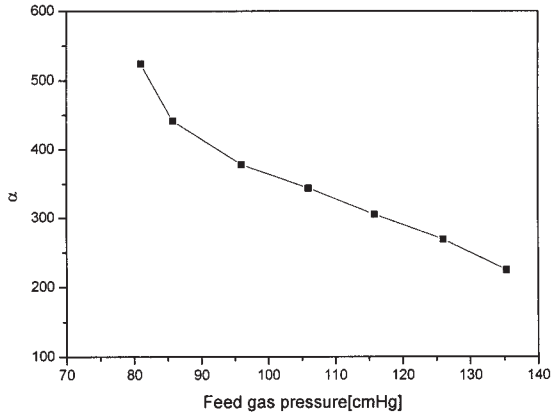

(b)

Figure 3 Effect of the feed gas pressure on the permselectivity of CO_2 over CH_4 with pure gas: (a) R_{CO2} and R_{CH4} and (b) α (testing temperature = 20°C, carrier concentration = 3.47 mmol/g, composition of the NVP–AAm copolymer = 56:44 mol/mol).

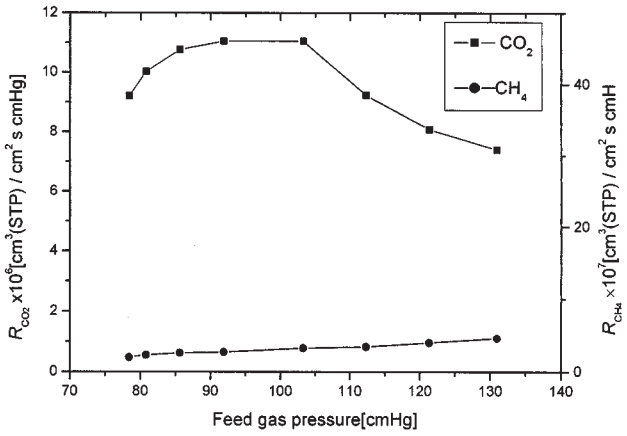

(a)

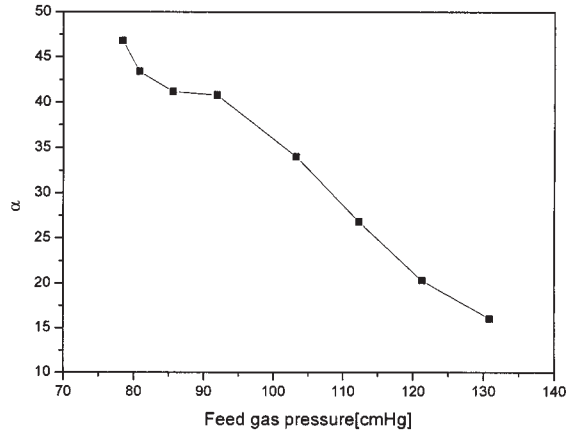

(b)

Figure 4 Effect of the feed gas pressure on the permselectivity of CO_2 over CH_4 with mixed gas: (a) R_{CO2} and R_{CH4} and (b) α (feed gas composition = 50 vol % CO_2 + 50 vol % CH_4, testing temperature = 20°C, carrier concentration = 3.47 mmol/g, composition of the NVP–AAm copolymer = 56:44 mol/mol).

TABLE I
Comparison of the Permselectivity of the Membranes Obtained in This Study with Those of Other Fixed Carrier Membranes in the Literature

Membrane	System	R_{CO2} [cm^3(STP)/cm^2 s cmHg]	α	P_{CO2} (atm)	Reference
Polymerized membrane from disopropylamine	CO_2/CH_4, 3.5 vol % CO_2	9.6×10^{-5}	11.5	1	6
Poly[2-(*N*,*N*-dimethyl)aminoethyl methacrylate]	CO_2/N_2, 58 vol % CO_2	5×10^{-6}	70	0.58	7
Polyethylenimine/poly(vinyl alcohol)	CO_2/N_2, 34.4 vol % CO_2	$<2 \times 10^{-6}$	50	0.34	8
Poly[2-(*N*,*N*-dimethyl)aminoethyl methacrylate-*co*-acrylonitrile]	Pure CO_2 and N_2	10^{-9}–10^{-8}	42–54	1	9
Poly(*N*-vinyl-γ-sodium aminobutyrate-*co*-sodium acrylate)	Pure CO_2 and CH_4	6.12×10^{-6}	524.4	1.06	This study
Poly(*N*-vinyl-γ-sodium aminobutyrate-*co*-sodium acrylate)	CO_2/CH_4, 50 vol % CO_2	9.20×10^{-6}	46.8	0.52	This study

brane absorbing CH_4 did not display any new band or any shift of bands, this indicated that the membrane did not react with CH_4. Therefore, the transport of CO_2 in the membrane followed the facilitated transport mechanism, whereas CH_4 transport in the membrane followed simple dissolution and diffusion.

Figure 5 shows that in the humidified membrane, CO_2 was transformed into the small and easy-to-move ion HCO_3^-. To further prove this, the dry polyester textile, which was the substrate of the PS ultrafiltration membrane, and the wet polyester textile absorbing CO_2 were also investigated by FTIR with attenuated total reflectance techniques, as shown in Figure 6. The two spectra were almost same; the substrate absorbing CO_2 did not display the HCO_3^- band at 1400 and 997 cm^{-1}. This indicated that the HCO_3^- arising from the reaction of CO_2 and water without carriers was too little to be detected by FTIR.

Therefore, it could be deduced that the carriers in the membrane could react with CO_2 reversibly, and this facilitated the transport of CO_2. At the same time, the carriers in the humidified membrane accelerated the transformation of CO_2 into HCO_3^-, which also promoted the permeation of CO_2.

In addition, the high polarity arising from the polar groups in the membrane diminished the solubility of the nonpolarity component CH_4, which was helpful for increasing R_{CO2} and α. From the standpoint of gas diffusion, the membrane was swollen by water brought by the sweep and feed gas. The diffusion coefficient was enhanced by the decrement of the movement resistance. Furthermore, gas could diffuse through the water bridge when the water concentration in the membrane was high.

As can be seen in Figure 3(a), R_{CO2} had a maximal value against the CO_2 partial pressure (P_{CO2}). In the low-pressure region ($P_{CO2} < 95$ cmHg), R_{CO2} increased with the increase in P_{CO2}. This was because when the casting solution was drying, the nonpolar groups of the macromolecule assembled on the surface of the casting solution. Thus, on the membrane surface, a very thin layer of inert groups was formed. Both CO_2 and CH_4 permeated this layer by diffusion. The inert layer could be destroyed by CO_2 with in-

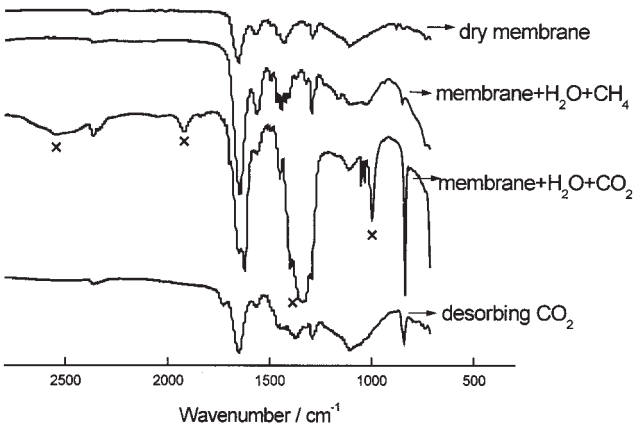

Figure 5 FTIR spectra of the dry membrane, the membrane absorbing CO_2, the membrane absorbing CH_4, and the membrane desorbing CO_2.

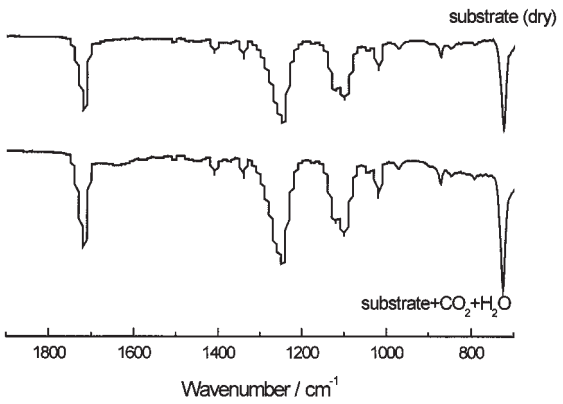

Figure 6 FTIR spectra of the wet polyester textile absorbing CO_2 and the dry polyester textile.

creasing pressure. Consequently, R_{CO2} increased with P_{CO2} in the low-pressure region and reached a maximal value. When the pressure was higher than 95 cmHg, R_{CO2} decreased with the increase in P_{CO2} because of the saturation of carriers in the membrane. Figure 3 also shows that R_{CH4} had a slow increase with the increase in the pressure of the feed gas. However, the reason for the increase in R_{CH4} is not very clear and will be sought in future research. The selectivities of CO_2/CH_4 decreased with increasing pressure of the feed gas.

Effects of various metal-ion crosslinkers on the properties of the membranes

Crosslinking is an effective and convenient method for improving the gas-transport properties of polymeric membranes.[14] Crosslinking membranes can improve the permselectivity and provide better stability. However, crosslinking has been shown to result in a significant decrease in the gas permeability. In this work, the prepared membranes were crosslinked with various metal ions, and the effects of the crosslinkers on the performances of the membranes were investigated.

Figure 7 shows the effect of the feed gas pressure on the permselectivities of the crosslinked membranes. In most cases, the permeation rate of the crosslinked membranes was lower than that of the uncrosslinked membrane. In comparison with that of the uncrosslinked membrane, the selectivity decrease of the crosslinked membrane with pressure was gentle. The selectivities of the crosslinked membranes were higher in the higher pressure region and lower in the lower pressure region. This was caused by the crosslinking between the membrane and metal ions. Crosslinking formed the metal chelate compound, which made the membrane more dense and led to a lower permeation rate. However, at the same time, crosslinking occurred at the expense of consuming the carrier (the secondary amine and carboxylate ion), and this resulted in not only a lower permeation rate but also decreased selectivity in the lower pressure region. Although the uncrosslinked membrane was easier to plasticize with CO_2 than the crosslinked membrane in the higher pressure region, this resulted in higher selectivity of the crosslinked membranes in the higher pressure region.

Among all the crosslinked membranes, the membrane crosslinked with calcium ion possessed the highest selectivity, the membranes crosslinked with magnesium and aluminum ions took second place, and the membranes crosslinked with transition-metal ions were the lowest. Calcium ions had a weak ability to chelate with the membrane, the ability of chelation between the transition-metal ions and the membrane was strong, and magnesium and aluminum ions were intervenient between calcium ions and transition-metal ions. Thus, the residual carriers in the membrane crosslinked with calcium ions were more than those of other membranes, and this caused its superior selectivity in comparison with other membranes. The selectivities of the membranes crosslinked with different transition-metal ions followed the famous Walliams–Irving sequence (Co^{2+}, $Fe^{2+} > Ni^{2+} < Cu^{2+} > Zn^{2+}$) of low-molecular-weight ligands on the

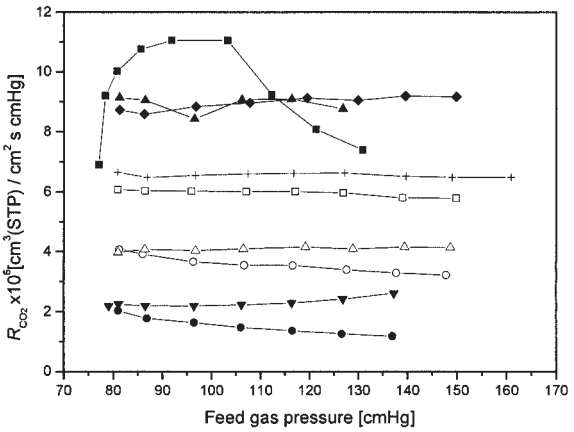

(a)

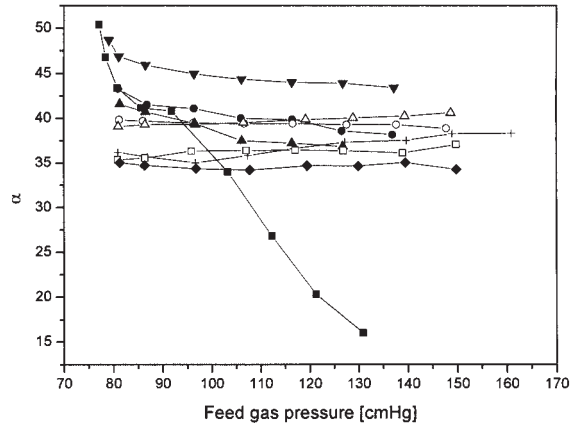

(b)

Figure 7 Effect of the feed gas pressure on the permselectivity of the crosslinked membrane with various metal ions: (a) R_{CO2} and (b) α for (■) the uncrosslinked membrane, (▼) the membrane crosslinked with Ca^{2+}, (●) the membrane crosslinked with Mg^{2+}, (○) the membrane crosslinked with Ni^{2+}, (△) the membrane crosslinked with Al^{3+}, (▲) the membrane crosslinked with Cu^{2+}, (+) the membrane crosslinked with Co^{2+}, (□) the membrane crosslinked with Fe^{3+}, and (♦) the membrane crosslinked with Zn^{2+} (feed gas composition = 50 vol % CO_2 + 50 vol % CH_4, carrier concentration before crosslinkage = 3.47 mmol/g, composition of the NVP–AAm copolymer = 56:44 mol/mol, testing temperature = 25°C).

whole,[15] but not exactly so. Because a metal chelate compound changes the molecular structure of a polymer, the situation is more complicated than that for a low molecular weight.

In contrast with the selectivity, the permeation rate of the membranes crosslinked with transition-metal ions was higher than that of other crosslinked membranes. This was due to two reasons. On the one hand, the formation of a metal chelate compound impeded the compact pileup of the polymer segment. On the other hand, the calcium and magnesium mainly chelated with carboxylate ions, whereas the transition-metal ions preferred to chelate with the secondary amine.[16] The chemical bonds between calcium and magnesium ions and carboxylate ions were electrovalent bonds, whereas those between the transition-metal ions and secondary amine were coordinate bonds. The difference in the chemical bonds between the metal ions and active groups led to the fact that the membrane containing an amine chelate compound was a little looser than the membrane containing a carboxylate-ion chelate compound.

Effect of the carrier concentration on the composite membrane performance

The concentration of the carriers could be increased by an increase in the hydrolysis degree. Therefore, it was necessary to determine the hydrolysis behavior of the NVP–AAm copolymer before the effect of the carrier concentration on the membrane performance was studied. Through changes in the alkali concentration, hydrolysis reaction temperature, and time, the hydrolysis degree could be changed, and this led to changes in the carrier concentration. Figure 8 shows the effects of the reaction conditions on the carrier concentration. With increasing alkali concentration and temperature, the activity of the reactive groups increased, and the hydrolysis rate was quickened; this led to an increase in the carrier concentration. With increasing reaction time, the carrier concentration increased remarkably during the initial stages, and then the curve became gentle.

Table II shows the effects of the carrier concentrations on the composite membrane performance. Both α and R_{CO2} had a maximum against the carrier concentration. This was because, on the one hand, the enhancement of the carrier concentration improved the facilitated transport of CO_2. On the other hand, the introduction of more carboxylate ions into the membrane (see Fig. 1) resulted in high polarity, and the high polarity of the molecules or functional groups led to net forces of attraction between the macromolecules, which reduced the d-spacing[17,18] and free volume. Furthermore, the crystallinity of the membrane was also increased with increasing carboxylate ions. These effects brought about the maximum of α and R_{CO2}.

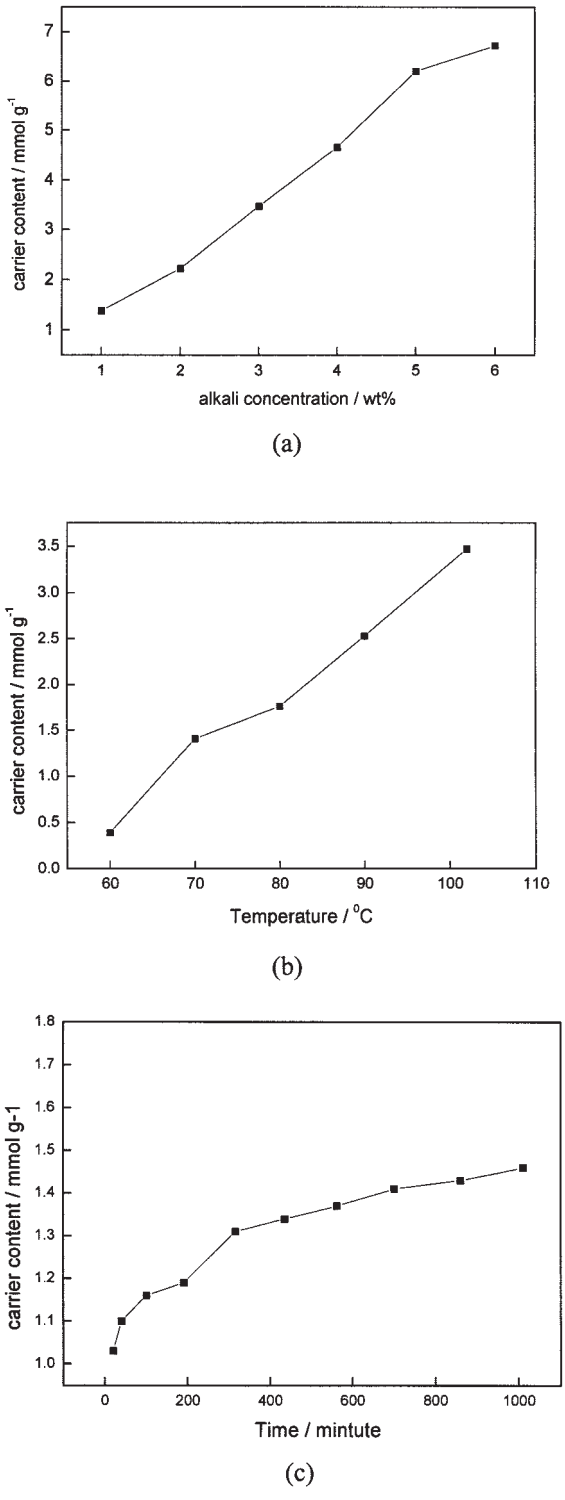

Figure 8 Effects of the hydrolysis reaction conditions on the carrier concentration: (a) temperature = 102°C and time = 11.5 h, (b) alkali concentration = 3% and time = 11.5 h, and (c) temperature = 70°C and alkali concentration = 3%.

Stability testing of the crosslinked membrane

From a practical point of view, a stability test was needed. Figure 9 shows the stability test of the

TABLE II
Effects of the Carrier Content on the Composite Membrane Performance

Carrier content (mol %)	α	$R_{CO2} \times 10^6$ [cm^3 (STP)/cm^2 s] cmHg	$R_{CH4} \times 10^7$ [cm^3 (STP)/cm^2 s cmHg]	*d*-spacing (Å)	Crystallinity (%)
0.39	33.1	5.32	1.60	9.8176	20.5
1.38	33.8	5.75	1.70	9.7708	21.2
2.22	35.1	6.99	1.99	9.9500	24.1
3.47	39.3	11.28	2.87	9.6887	24.2
4.65	38.3	7.83	2.04	9.4812	36.3
6.2	36.2	5.10	1.40	9.4007	34.3

Feed gas pressure = 86.5 cmHg; feed gas composition = 50 vol % CO_2 + 50 vol % CH_4; testing temperature = 20°C; composition of the NVP–AAm copolymer = 56:44 mol/mol.

crosslinked membrane with Ni^{2+} ion. R_{CO2} decreased 40%, and α increased 20% in the first 50 h. Then, both α and R_{CO2} remained constant. This indicated that the membrane developed in this work was stable.

CONCLUSIONS

VSA–SA/PS composite membranes were prepared for the separation of CO_2/CH_4. The ideal α and R_{CO2} values obtained at 20°C were 524.4 and 6.12×10^{-6} cm^3(STP)/cm^2 s cmHg, respectively, when the pressure in the feed gas was 1.06 atm.

The transport mechanism of CO_2 in the membrane was studied by FTIR with attenuated total reflectance techniques. The carriers could react with CO_2 reversibly and accelerate the transformation of CO_2 into HCO_3^- in the humidified membrane, and this facilitated the permeation of CO_2.

In comparison with the uncrosslinked membrane, the gas permeances of the crosslinked membranes were lower, and the selectivities were higher in the higher pressure region and lower in the lower pressure region. Among the crosslinked membranes, the membranes crosslinked with calcium, magnesium, and aluminum ions possessed higher α values and lower R_{CO2} values, whereas the membranes crosslinked with transition-metal ions had higher R_{CO2} values but lower α values.

Both α and R_{CO2} had a maximum against the carrier concentration. This was because the various carrier concentrations led to the variation of not only facilitated transport but also *d*-spacing and crystallinity.

The crosslinked membranes prepared in this work had good stability. Both the selectivity and permeation rate remained almost constant after a certain operating time.

NOMENCLATURE

α	selectivity of CO_2 over CH_4
AAm	acrylamide

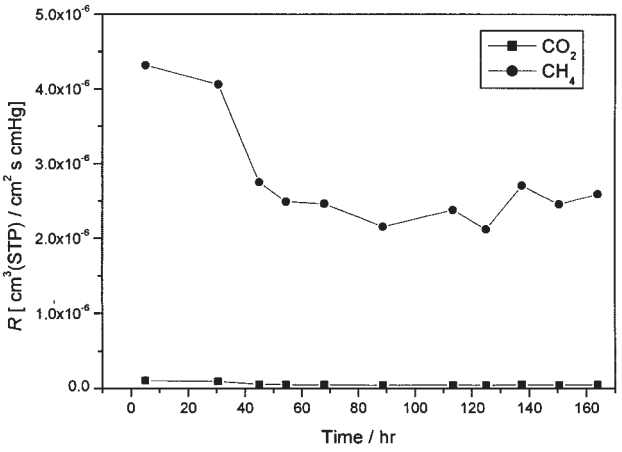

(a)

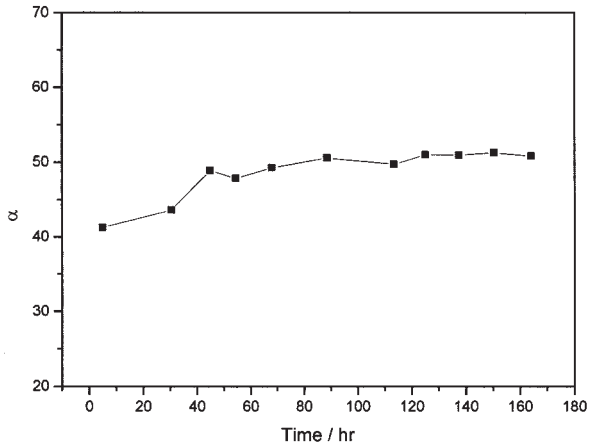

(b)

Figure 9 Stability of the crosslinked membrane: (a) *R* and (b) α (feed gas pressure = 56.3 cmHg, feed gas composition = 19 vol % CO_2 + 81 vol % CH_4, carrier concentration before crosslinkage = 3.47 mmol/g, composition of the NVP–AAm copolymer = 66:34 mol/mol, testing temperature = 20°C, crosslinker = Ni^{2+}, crosslinking time = 1 min).

ΔP_i	pressure difference between the upstream and downstream sides of the membrane (cmHg)
FTIR	Fourier transform infrared
N_i	flux [cm^3(STP)/cm^2 s]
NVP	*N*-vinylpyrrolidone
P_{CO2}	CO_2 partial pressure of feed gas (atm or cmHg)
PS	polysulfone
R_{CH4}	permeation rate of CH_4 [cm^3(STP)/cm^2 s cmHg]
R_{CO2}	permeation rate of CO_2 [cm^3(STP)/cm^2 s cmHg]
R_i	permeation rate [cm^3(STP)/cm^2 s cmHg]
VSA–SA	poly(*N*-vinyl-γ-sodium aminobutyrate-*co*-sodium acrylate)

References

1. Schell, W. J. J Membr Sci 1985, 22, 217.
2. Stern, S. A. J Membr Sci 1994, 94, 1.
3. Robeson, L. M. J Membr Sci 1991, 62, 165.
4. Way, J. D.; Noble, R. D. In Membrane Handbook; Ho, W. S.; Sirkar, K. K., Eds.; Van Nostrand Reinhold: New York, 1992; p 833.
5. Guha, A. K.; Majumdar, S.; Sirkar, K. K. Ind Eng Chem Res 1990, 29, 2093.
6. Matsuyama, H.; Hirai, K.; Teramoto, M. J Membr Sci 1994, 92, 257.
7. Matsuyama, H.; Teramoto, M.; Sakakura, H. J Membr Sci 1996, 114, 193.
8. Matsuyama, H.; Terada, A.; Nakagawara, T.; Kitamura, Y. M. J Membr Sci 1999, 163, 221.
9. Yoshikawa, M.; Fujimoto, K.; Kinugawa, H.; Kitao, T.; Ogata, N. Chem Letter 1994, 243.
10. Quinn, R.; Appleby, J. B.; Pez, G. P. J Membr Sci 1995, 104, 139.
11. Zhang, Y.; Wang, Z.; Wang, S. C. Chem Letter 2002, 430.
12. Massarat, B. S. O.; Dakroury, A. Z.; Mokhtar, S. K. Polym Bull 1992, 28, 181.
13. Yeom, C. K.; Lee, S. H.; Lee, J M. J Appl Polym Sci 2000, 78, 179.
14. Ismail, A. F.; Lorna, W. Sep Purif Technol 2002, 27, 173.
15. Ciardelli, F.; Tsuchida, E.; Wohrle, D. Macromolecule–Metal Complexes; Springer-Verlag: Berlin, 1996; p 64.
16. Greenwood, N. N.; Earnshaw, A. Chemistry of the Elements, 2nd ed.; Reed Educational and Professional: Oxford, 1997; p 905.
17. Stern, S. A.; Mi, Y.; Yamamoto, H. J Polym Sci Part B: Polym Phys 1989, 27, 1887.
18. Kim, T. H.; Koros, W. J.; Husk, G. R. Sep Sci Technol 1988, 23, 1611.